FRET Analysis of Protein-Lipid Interactions

Galyna Gorbenko and Paavo K.J. Kinnunen

Abstract Förster resonance energy transfer (FRET) is an old but constantly developing spectroscopic tool possessing enormous potential for studies on structure and dynamics of biological macromolecules and their assemblies. One of the main advantages of FRET technique is the possibility of measuring the nanometer-scale distances between donor and acceptor fluorophores. This chapter highlights some aspects of FRET-based monitoring of intermolecular interactions in membrane systems. Analytical model of energy transfer between membrane-associated donors and acceptors randomly distributed over parallel planes separated by a fixed distance is presented. The factors determining the efficiency of energy transfer are considered with special attention to orientational behavior of the donor emission and acceptor absorption transition dipoles. It is demonstrated that FRET can provide proof for specific orientation of the protein molecule relative to lipid-water interface. The applications of FRET to quantification of protein-lipid binding parameters and membrane position of protein fluorophores are exemplified. It is illustrated how FRET may help in obtaining evidence for protein aggregation in a membrane environment and domain formation.

Keywords Domain formation · Förster resonance energy transfer · Protein aggregation · Protein-lipid interactions · Structural and binding parameters

G. Gorbenko
Department of Biological and Medical Physics, V.N. Karazin Kharkov National University, Svobody Sq. 4, 61022 Kharkov, Ukraine

P.K.J. Kinnunen (✉)
Department of Biomedical Engineering and Computational Science, School of Science, Aalto University, Otakaari 3, 02150 Espoo, Finland
e-mail: paavo.kinnunen@aalto.fi

Y. Mély and G. Duportail (eds.), *Fluorescent Methods to Study Biological Membranes*, Springer Ser Fluoresc (2013) 13: 115–140, DOI 10.1007/4243_2012_45,

Contents

1 Introduction

Förster resonance energy transfer is one of the most powerful fluorescence techniques and has found innumerable applications in biomedical research [1–3]. Due to explicit dependence on the distance between the fluorophores acting as energy donor and acceptor, FRET represents a unique tool for establishing nanometer-scale proximity relationships both in vivo and in vitro, thereby giving structural information complementary to that provided by other mighty physical methods, such as NMR, X-ray and neutron scattering, and electron and optical microscopy [4, 5]. FRET has proven to be especially powerful in structural characterization of a wide variety of macromolecular assemblies, biological membranes, in particular [3, 6–8]. The interactions between two major membrane constituents, proteins, and lipids have long been a focus of FRET studies, greatly contributing to understanding the mechanisms of the membrane binding of proteins [9, 10], conformational transitions of polypeptide chains in a membrane environment [11, 12], lipid-mediated protein aggregation [13, 14], domain formation [15, 16], etc. Among the principal advantages of FRET technique are (1) the possibility of experimentation within protein and lipid concentration range where most other methods appear powerless; (2) revealing the subtle peculiarities of protein-membrane interactions; (3) detection of small amounts of molecular clusters, unaccessible to other techniques; (4) the opportunity for obtaining information about the structural state of a protein and lipid bilayer under the same experimental conditions; and (5) high sensitivity and relative simplicity of the experiment.

This chapter is intended to give a concise overview of the possibilities provided by FRET in the studies of protein-lipid interactions. Along with considering the fundamental principles of FRET, basic formalism for description of energy transfer in membranes, and some problems encountered in quantification of FRET data, we present some examples illustrating how steady-state FRET can be used to determine protein-membrane binding characteristics, orientation of the protein molecule relative to lipid-water interface, its transverse bilayer location, and aggregation state.

2 Basics of FRET

Förster resonance energy transfer (FRET) is a process by which energy is passed between molecules over long distances (from about 1 to 10 nm) [17]. The donor molecule, which must be a fluorophore, is excited by incident light and transfers the absorbed energy nonradiatively to the acceptor molecule, which, in the majority of cases, is capable of fluorescing. Since energy transfer occurs without emitting a photon and results from long-range dipole-dipole interactions between the donor and acceptor, it seems inaccurate to decipher the frequently used acronym FRET as fluorescence resonance energy transfer. Instead, according to the recommendations of IUPAC, it is more correct to use the term "Förster resonance energy transfer," paying tribute to the German scientist Theodor Förster who first proposed the mechanism of this phenomenon.

Förster developed a theoretical basis of FRET using both classical physics and quantum mechanics approaches [18]. Classical physics considers the transfer of excitation energy from one molecule to another as resulting from the resonance interactions between closely spaced oscillating dipoles, similar to two oscillating pendulums that are mechanically coupled. Quantum mechanical description of FRET is based on Fermi's golden rule which is used to calculate the probability of transition from initial state $\boldsymbol{i}$ ($\Psi_i = \Psi_{D_1}\Psi_{A_0}$, donor is in an excited state, while acceptor is in a ground state,) to final state $\boldsymbol{f}$ ($\Psi_f = \Psi_{D_0}\Psi_{A_1}$, donor is in a ground state, acceptor is in an excited state) due to a perturbation caused by light absorption:

$$\frac{dP_f}{dt} = \frac{1}{2\hbar^2}\left|\langle\Psi_f|\tilde{\mu}|\Psi_i\rangle E_0\right|^2 \tag{1}$$

The rate constant of energy transfer between donor and acceptor separated by a distance R is given by the following equations:

$$k_T(\nu) \propto \left|\left\langle\Psi_{D_1}\Psi_{A_0}\middle|\tilde{V}\middle|\Psi_{D_0}\Psi_{A_1}\right\rangle\right|^2 \tag{2}$$

$$\tilde{V} = \frac{1}{\varepsilon}\left[\frac{(\tilde{\mu}_D\cdot\tilde{\mu}_A)}{R^3} - 3\frac{(\tilde{\mu}_D\cdot R)(R\cdot\tilde{\mu}_A)}{R^5}\right] \tag{3}$$

$$k_T(\nu) \propto \frac{\kappa^2}{\varepsilon^2 R^6}\left|\langle\Psi_{D_1}|\tilde{\mu}_D|\Psi_{D_0}\rangle\right|^2\left|\langle\Psi_{A_0}|\tilde{\mu}_A|\Psi_{A_1}\rangle\right|^2 \tag{4}$$

$$\left|\langle\Psi_{A_0}|\tilde{\mu}_A|\Psi_{A_1}\rangle\right|^2 \propto \frac{\varepsilon_A}{\nu}, \quad \left|\langle\Psi_{D_1}|\tilde{\mu}_D|\Psi_{D_0}\rangle\right|^2 \propto \frac{1}{\nu^3\tau_R} = \frac{\varphi_D}{\nu^3\tau_D} \tag{5}$$

Here $\tilde{V}$ is the operator for dipole-dipole interaction between donor and acceptor. Remarkably, both classical and quantum mechanical theories of energy transfer yield similar final expression for the rate constant of FRET:

$$k_T \propto \frac{\kappa^2 \varphi_D}{n^4 R^6 \tau_D} \int \frac{\varepsilon_A(\nu) f_D(\nu)}{\nu^4} d\nu = \frac{\kappa^2 \varphi_D}{R^6 \tau_D} J \tag{6}$$

Förster theory predicts that the rate of energy transfer depends on the donor-acceptor distance (R); quantum yield of the donor in the absence of acceptor (φ_D); refractive index of the medium (n), which is typically taken as 1.4 for biomolecules in aqueous solution; donor lifetime in the absence of acceptor (τ_D); orientation factor (κ^2), determined by the relative orientation of the donor and acceptor dipoles; and overlap between donor emission ($f_D(\nu)$) and acceptor absorption spectra ($\varepsilon_A(\nu)$). By combining distance-independent terms, the expression for rate constant can be rewritten as

$$k_T = \frac{1}{\tau_D} \left(\frac{R_0}{R} \right)^6; \quad R_0^6 = \frac{\kappa^2 \varphi_D}{n^4} \left(\frac{9,000(\ln 10)}{128 \pi^5 N_A} \right) \int \frac{\varepsilon_A(\nu) f_D(\nu)}{\nu^4} d\nu \tag{7}$$

here, R_0 is an important parameter called Förster distance. The efficiency of energy transfer (E) is the fraction of photons absorbed by the donor that are transferred to the acceptor, which is given by the ratio of the transfer rate to the total decay rate of the donor. On the other hand, transfer efficiency can be represented as a function of Förster radius and donor-acceptor distance:

$$E = \frac{k_T}{k_T + \tau_D^{-1}} = \frac{R_0^6}{R_0^6 + R^6} \tag{8}$$

As follows from this equation, Förster radius defines the distance at which energy transfer efficiency is 50%, and the transfer rate is equal to the donor decay rate. This is a characteristic parameter of each donor-acceptor pair, which typically falls in the 2–6-nm range [19]. A very steep distance dependence of FRET efficiency, being inversely proportional to the sixth power of donor-acceptor separation, along with the fact that Förster radii of most donor-acceptor pairs are comparable to the size of proteins and membranes, makes FRET the technique of choice, a spectroscopic ruler, to quantify spatial relationships between intrinsic and extrinsic fluorophores in biological macromolecules and their assemblies [20].

3 FRET in Membranes

To determine FRET transfer efficiency experimentally, three different approaches are generally used, based on measuring the decrease of donor fluorescence intensity (I_D) or average lifetime ($\langle \tau_D \rangle$) in the presence of acceptor (I_{DA},$\langle \tau_{DA} \rangle$):

$$E = 1 - \frac{\varphi_{DA}}{\varphi_D} = 1 - \frac{I_{DA}}{I_D}; \quad E = 1 - \frac{\langle \tau_{DA} \rangle}{\langle \tau_D \rangle} \tag{9}$$

or enhancement of acceptor fluorescence (I_A) after donor excitation:

$$E = \frac{\varepsilon_A(\lambda_D^{ex}) C_A}{\varepsilon_D(\lambda_D^{ex}) C_D} \left(\frac{I_{AD}(\lambda_A^{em})}{I_A(\lambda_A^{em})} - 1 \right) \tag{10}$$

Here $I_A(\lambda_A^{em})$, $I_{AD}(\lambda_A^{em})$ are acceptor fluorescence intensities in the absence and presence of donor at emission wavelength λ_A^{em}; $\varepsilon_D(\lambda_D^{ex})$, $\varepsilon_A(\lambda_D^{ex})$ are extinction coefficients of the donor and acceptor at the donor excitation wavelength λ_D^{ex}; and C_D,C_A are the concentrations of donor and acceptor, respectively.

It is important to emphasize that the simple relationship 8 describing distance dependence of energy transfer efficiency is valid only for one donor and one acceptor separated by a fixed distance, as may be the case, for instance, in labeled proteins. However, this relationship is inapplicable for donors and acceptors distributed in solution or in a membrane phase. In these cases, more complex expressions are required, which are commonly derived from averaging the transfer rate over multiple donor-acceptor pairs. This problem is addressed in a number of models developed for two-dimensional systems [21–27]. To illustrate principal features of FRET in membranes, we consider here one of these models proposed by Fung and Stryer for the case of donors and acceptors randomly distributed in a plane [21]. It should be noted in this regard that if the diameter of membrane vesicles is more than twofold greater than Förster radius, the curvature effect is negligible so that energy transfer can be considered as occurring in a plane. This is valid for the majority of membrane systems since the Förster distances do not exceed 10 nm, while the radius of vesicles formed by the model or isolated native membranes is usually greater than 20 nm. In terms of the model of Fung and Stryer, the efficiency of energy transfer is given by

$$E = 1 - \int_0^{\infty} \exp(-\lambda) \exp\left(-C_a^s S(\lambda)\right) d\lambda \tag{11}$$

$$S(\lambda) = \int_{r_c}^{\infty} \left[1 - \exp\left(-\lambda \left(\frac{R_o}{R} \right)^6 \right) \right] 2\pi R dR, \quad \lambda = \frac{t}{\tau_D} \tag{12}$$

where τ_D is the lifetime of excited donor in the absence of acceptor, r_c is the distance of closest approach between the donor and acceptor, and C_a^s is the concentration of acceptors per unit area related to the molar concentrations of lipids accessible to acceptor (L_a) and bound acceptor (B_a):

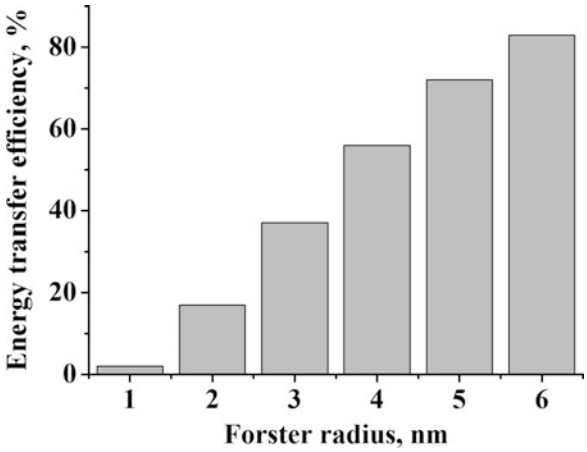

Fig. 1 Efficiencies of energy transfer between donors and acceptors randomly distributed in a plane. Acceptor surface density is one acceptor molecule per 100 lipid molecules. The distance of closest approach between donor and acceptor is taken as 0.8 nm

$$C_a^s = \frac{B_a}{L_a \sum f_i S_i} \tag{13}$$

Here f_i, S_i are the fraction and mean surface area of the *i-th* membrane constituent.

Shown in Fig. 1 are energy transfer efficiencies calculated by numerical integration of the Eq. 11. It can be seen that a relatively low acceptor surface density (one acceptor molecule per 100 lipid molecules) results in rather high energy transfer at Förster radii exceeding 2 nm. Remarkably, the above formalism is applicable to various geometric conditions of energy transfer. Particularly, for donors and acceptors uniformly distributed over different planes separated by a distance d_a (Fig. 2a), Eq. 12 takes the form

$$S(\lambda) = \int_{d_a}^{\infty} \left[1 - \exp\left(-\lambda\left(\frac{R_o}{R}\right)^6\right)\right] 2\pi R dR \tag{14}$$

Another possible configuration involves one donor plane located at a distance d_c from the membrane center and two acceptor planes with identical C_a^s, separated by a distance d_t (Fig. 2b). Given that for the outer acceptor plane, $d_a = |d_c - 0.5d_t|$, while for the inner plane, $d_a = d_c + 0.5d_t$, the following relationships hold:

$$S_1(\lambda) = \int_{|d_c - 0.5d_t|}^{\infty} \left[1 - \exp\left(-\lambda\left(\frac{R_o}{R}\right)^6\right)\right] 2\pi R dR \tag{15}$$

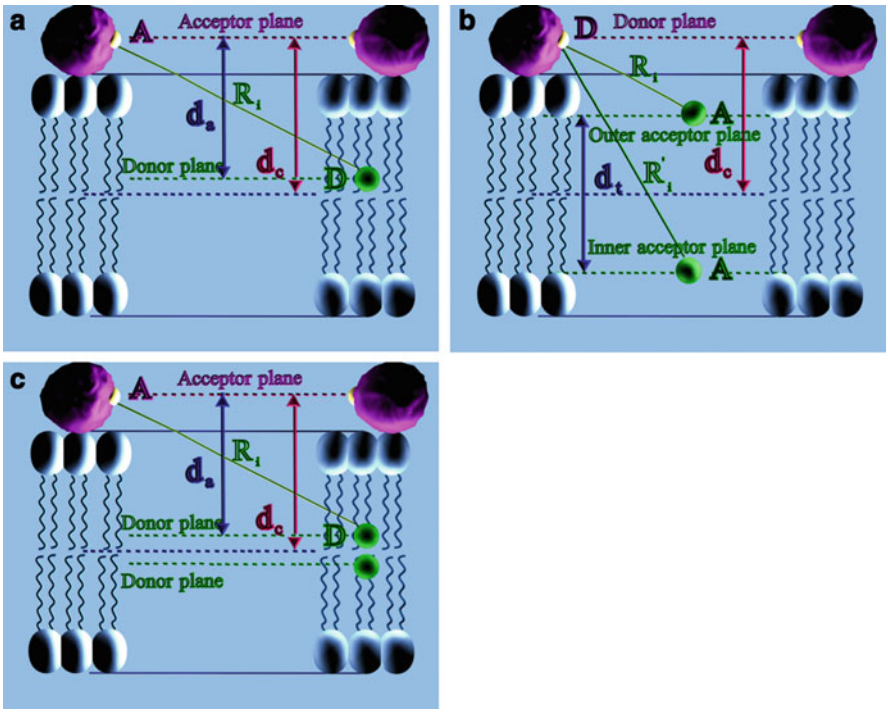

Fig. 2 Schematic representation of planar arrangement of donors and acceptors in a lipid bilayer

$$S_2(\lambda) = \int_{d_c+0.5d_t}^{\infty} \left[1 - \exp\left(-\lambda\left(\frac{R_o}{R}\right)^6\right)\right] 2\pi R dR \tag{16}$$

$$E = 1 - \int_0^{\infty} \exp(-\lambda)\exp\left[-C_a^s(S_1(\lambda) + S_2(\lambda))\right] d\lambda \tag{17}$$

where S_1 and S_2 are the quenching contributions describing energy transfer to the outer and inner acceptor planes, respectively. Alternatively, if there exist one acceptor plane located at a distance d_c from the membrane center and two donor planes separated by a distance d_t (Fig. 2c), energy transfer efficiency can be written as

$$E = 1 - 0.5 \times \left(\int_0^{\infty} \exp(-\lambda)\exp\left[-C_a^s S_1(\lambda)\right] d\lambda + \int_0^{\infty} \exp(-\lambda)\exp\left[-C_a^s S_2(\lambda)\right] d\lambda \right) \tag{18}$$

Next, it seems of importance to illustrate what kind of information can be obtained by applying the above uniform distribution formalism to the analysis of FRET in protein-lipid systems. To this end, we will consider some representative examples of experimental design and data treatment strategy, concerning protein (1) orientation relative to lipid-water interface, (2) membrane binding parameters, (3) the depth of bilayer penetration, (4) aggregation state, and (5) effect on lipid lateral distribution.

4 FRET Study of Orientational Behavior of Membrane-Bound Proteins

As follows from the above considerations, the efficiency of FRET is a function of the donor-acceptor distance, the donor quantum yield, overlap of the donor emission and acceptor absorption spectra, and relative orientation of the donor and acceptor transition dipoles. Of these, the most problematic parameter is the orientation factor κ^2 defined as [28]:

$$\kappa^2 = (\sin\theta_D \sin\theta_A \cos\varphi - 2\cos\theta_D \cos\theta_A)^2 \tag{19}$$

where θ_D and θ_A are the angles between the donor emission ($\boldsymbol{D}$) or acceptor absorption ($\boldsymbol{A}$) transition moments and the vector $\boldsymbol{R}$ joining the donor and acceptor and φ is the dihedral angle between the planes ($\boldsymbol{D}$, $\boldsymbol{R}$) and ($\boldsymbol{A}$, $\boldsymbol{R}$). Orientation factor can vary from 0 to 4, the minimum value corresponds to perpendicularly oriented donor and acceptor dipoles, while the maximum one characterizes the case when these dipoles are parallel and identically directed [19]. It is a common practice in FRET studies to use the isotropic value of orientation factor, 0.67, which is valid in the case when donors and acceptors can adopt all orientations (isotropic condition) in a time short compared to the transfer time (dynamic averaging condition) [28]. However, in a highly anisotropic membrane environment, rotational mobility of donors and acceptors is usually restricted, and the isotropic condition is hardly satisfied. Besides, if the donor and acceptor dipoles exhibit certain preferable orientations, for instance, when protein-lipid interactions involve specific binding sites, κ^2 value may substantially differ from 0.67. Such an uncertainty in the choice of orientation factor is regarded as the main source of uncertainty in the quantitative interpretation of FRET data. In the following, we will consider some possible ways for circumventing this problem.

First example is intended to illustrate how FRET can help to answer the question of whether there exists certain specific orientation of the protein molecule relative to lipid-water interface. This question has been addressed in our early study of lipid bilayer interactions of cytochrome *c*, a peripheral mitochondrial protein which plays important role in respiration process and apoptosis. Cytochrome *c* is a globular protein with the size about 3 nm, containing heme group located 1.5 nm from its

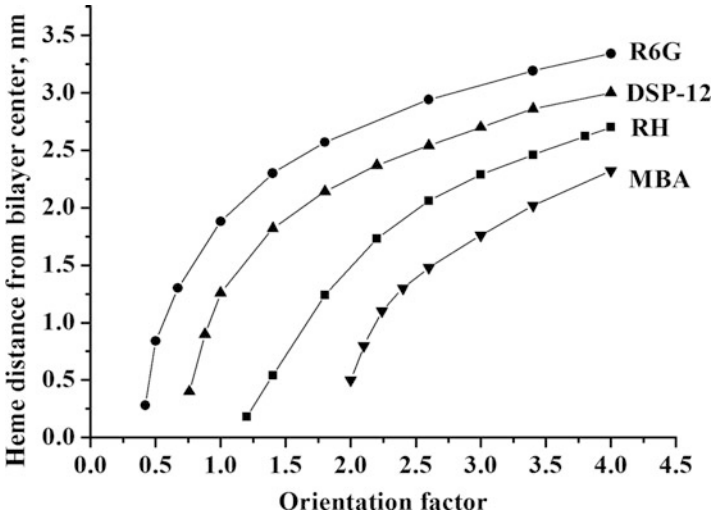

Fig. 3 Dependence of the distance between heme group of cytochrome *c* and membrane midplane on orientation factor

surface. This group is an effective energy acceptor for a number of fluorophores. We employed FRET technique to examine cytochrome *c* association with the model membranes, composed of zwitterionic lipid phosphatidylcholine (PC) and anionic lipid cardiolipin (CL) [29]. Several fluorescent probes, including (3-methoxybenzanthrone (MBA), *N*,*N*′-bishexamethylenrhodamine (RH), rhodamine 6G (R6G), and 4-(dimethylaminostyryl)-1-dodecylpiridine (DSP-12)), were used as donors, while heme group of the protein was recruited as acceptor. The donors are distributed between the outer and inner bilayer leaflets, thus forming two donor planes, separated by a certain distance d_t, while protein molecules are supposed to reside at the outer membrane side, forming one acceptor plane, located at a distance d_c from the membrane center (Fig. 2c). In this case, relative quantum yield of the donor can be written as the sum of two terms, where lower integration limits correspond to the separation of acceptor plane from the outer and inner donor planes. The data treatment strategy involved fitting of the relative quantum yields calculated by numerical integration of the Eqs. 15, 16 and 18 to those measured experimentally with the distance between the acceptor plane and membrane center (d_c) as the optimizing parameter. This procedure was repeated for all FRET profiles with κ^2 being varied in the widest possible range, from 0 to 4. As a result, we obtained numerous sets of two parameters—acceptor distance from the bilayer midplane and orientation factor – providing the best fit of the experimental data. Several features of $d_c(\kappa^2)$ dependencies are worthy of mention. As can be seen in Fig. 3, for each of the employed donors, there exists certain minimum κ^2 value characterizing the situation when heme groups reside at the bilayer midplane ($d_c = 0$), and maximum heme distance from the bilayer center ($d_c^{\max}$), estimated at $\kappa^2 = 4$. In the case of random reorientation of donors and acceptors, one should expect the intersection or

closing of the plots $d_c(\kappa^2)$, obtained for different donors, at a point, corresponding to the isotropic value of orientation factor ($\kappa^2 = 0.67$) and actual heme separation from the bilayer midplane, since this parameter appears to be invariant over a series of donors. The absence of such an intersection implies that orientation of heme dipole cannot be considered as random. Another support for this assumption comes from the observation that for some donors, specifically, MBA and RH, the minimum possible κ^2 value is greater than 0.67. Taken together, these findings suggest that there exists certain specific orientation of the heme group relative to lipid-water interface. It is known that acidic and basic groups on the surface of cytochrome *c* molecule are segregated into two positively charged patches with negative patch between them [30]. The involvement of one of the positively charged patches in the interactions with lipids may account for specific protein disposition with respect to the membrane surface. This example demonstrates that uncertainty in the orientation factor value can be turned to our advantage by the proper experimental design, employing the donors distributed symmetrically between the outer and inner membrane leaflets and protein-associated acceptors. The observations, such as noncrossing dependencies of the acceptor distance from the membrane center on the orientation factor obtained for different donors and/or successful data fitting only for κ^2 exceeding the isotropic value, may serve as the indications for the existence of specific lipid-binding site on the surface of protein molecule.

Importantly, FRET can provide not only qualitative but also quantitative topological information about membrane-associated proteins. For instance, using a series of site-directed cysteine mutants fluorescently labeled with AEDANS, Nazarov et al. succeeded in determining the topology and bilayer embedment of M13 major coat protein in dioleoylphosphatidylcholine/dioleoyl phosphatidylglycerol (4:1 mol/mol) vesicles. The authors developed novel simulation-based fitting approach that was applied to analyzing the steady-state FRET between tryptophan as a donor and AEDANS as an acceptor. The tilt of the transmembrane helix of M13 major coat protein was found to be around 18° [31].

5 Membrane Location of Proteins Determined from FRET

One of the most widespread applications of FRET in membrane studies involves characterization of protein disposition in a lipid bilayer. Both analytical and numerical approaches have been used to obtain quantitative estimates for membrane embedment of a variety of structurally different proteins, as summarized in Table 1. It should be noted in this regard that the choice of a certain theoretical strategy for analyzing FRET data is dictated by specific structural features of the system under study, such as randomness of fluorophore distribution, size of the donor- or acceptor-bearing protein domain, and spatial relationships between donor and acceptor arrays. However, in all cases, the uncertainty in orientation factor value may substantially reduce or even eliminate the reliability of FRET estimates of the protein bilayer location. In view of this, we found it reasonable to briefly

Table 1 Illustrative examples of FRET-based evaluation of protein position in a membrane

Protein	Membrane	Structural information	Reference
GPI-anchored alkaline phosphatase (PLAP)	PC	The distance between PLAP and lipid-water interface is smaller than 1–1.4 nm	[32]
Acetylcholine receptor (AChR)	Native AChR-rich membrane	Minimum distance between Trp and Laurdan is ca. 1.4 nm	[33]
C-terminal sterile α motif (SAM) domain of human p73	PC, phosphatidic acid	Trp is located at 1.1–2 nm from the bilayer center	[34]
Perfringolysin	PC, cholesterol	Domain 1 is located ca. 11 nm above the membrane surface	[35]
Cytochrome b_5	PC	Heme moiety is located about 1.5 nm from the membrane surface, Trp is buried at the depth ca. 2 nm	[36]
α-toxin	PC, PG, cholesterol	Cys130 and Cys69 distances from polar/nonpolar transition region are ca. 0.8 and 8 nm, respectively	[37]
P-glycoprotein	PC, phosphatidylethanolamine	The distance of Cys residues from the lipid-water interface is ca. 3.1–3.5 nm	[38]
Hemoglobin	Red blood cell membrane	Distance between heme groups and 12-(9-anthroyl)stearic acid is ca. 4–6 nm	[39]
$(Ca^{2+} + Mg^{2+})$-ATPase	PC	Ca^{2+} binding sites of ATPase reside at 2 nm distance from the lipid-water interface	[40]
Acetylcholine receptor (AChR)	AChR membrane	Ethidium binding site is positioned ca. 5 nm from the membrane surface	[41]
G-protein	PC	Distances between protein α, β, and γ subunits and lipid headgroups are ca. 4.6, 3.8, and 3.7 nm, respectively	[42]
Epidermal growth factor (EGF)	Plasma membranes of epidermoid carcinoma cells	Amino terminus of EGF is about 6.7 nm away from the cell surface	[43]
Lysozyme	PC, PG	Average distance between Trp residues and bilayer center is ca. 2 nm	[44]
Cytochrome *c*	PC, CL	Heme distance from the bilayer midplane lies between 3.6 and 4 nm	[45]
M13 major coat protein	PC, PG	Trp separation from the membrane center is ca. 8.5 nm	[31]

describe here one approach to reducing this problem, based on the early work of Davenport et al. [46].

The applicability of Eq. 19 is limited to the case when the vectors $\boldsymbol{D}$ and $\boldsymbol{A}$ do not undergo any reorientation during the transfer time. Alternatively, Förster radius should be calculated using the dynamic average value of orientation factor $\left(\left\langle \kappa^2 \right\rangle\right)$. If the donor emission and acceptor absorption transition moments are symmetrically distributed within the cones about certain axes $\boldsymbol{D_x}$ and $\boldsymbol{A_x}$, $\left\langle \kappa^2 \right\rangle$ is given by [28]:

$$\begin{aligned}\left\langle \kappa^2 \right\rangle = {} & (\sin\Theta_D \sin\Theta_A \cos\Phi - 2\cos\Theta_D \cos\Theta_A)^2 \left\langle d_D^x \right\rangle \left\langle d_A^x \right\rangle \\ & + 1/3(1 - \left\langle d_D^x \right\rangle) + 1/3(1 - \left\langle d_A^x \right\rangle) \\ & + \cos^2\Theta_D \left\langle d_D^x \right\rangle \left(1 - \left\langle d_A^x \right\rangle\right) + \cos^2\Theta_A \left\langle d_A^x \right\rangle \left(1 - \left\langle d_D^x \right\rangle\right) \end{aligned} \tag{20}$$

where Θ_D and Θ_A are the angles made by the axes $\boldsymbol{D_x}$ and $\boldsymbol{A_x}$ with the vector $\boldsymbol{R}$, Φ is the angle between the planes containing the cone axes and the vector $\boldsymbol{R}$, and $\left\langle d_D^x \right\rangle$ and $\left\langle d_A^x \right\rangle$ are so-called axial depolarization factors:

$$\left\langle d_{D,A}^x \right\rangle = 3/2 \left\langle \cos^2 \psi_{D,A} \right\rangle - 1/2 \tag{21}$$

where $\psi_{D,A}$ are the cone half-angles. These factors are related to the steady-state (r) and fundamental (r_0) anisotropies of the donor and acceptor [28]:

$$d_{D,A}^x = \pm \left(r_{D,A}/r_{0D,A}\right)^{1/2} \tag{22}$$

When the donor and acceptor planar arrays are located at different levels across the membrane, separated by a distance d_a, multiple donor-acceptor pairs are involved in energy transfer, so that orientation factor appears to be a function of the donor-acceptor separation (R). Particularly, for the most probable membrane orientation of $\boldsymbol{D_x}$ and $\boldsymbol{A_x}$, parallel to the bilayer normal, the angles Θ_D and Θ_A made by $\boldsymbol{D_x}$ and $\boldsymbol{A_x}$ with $\boldsymbol{R}$ are equal and depend on the distance between donor and acceptor ($\Theta_A = \Theta_D = \theta$, $\theta = f(R)$). Under these circumstances, Eq. 20 can be rewritten in the form

$$\begin{aligned}\left\langle \kappa^2(\theta) \right\rangle = {} & \left\langle d_D^x \right\rangle \left\langle d_A^x \right\rangle \left(3\cos^2\theta - 1\right)^2 + 1/3\left(1 - \left\langle d_D^x \right\rangle\right) + 1/3\left(1 - \left\langle d_A^x \right\rangle\right) \\ & + \cos^2\theta \left(\left\langle d_D^x \right\rangle - 2\left\langle d_D^x \right\rangle \left\langle d_A^x \right\rangle + \left\langle d_A^x \right\rangle\right) \end{aligned} \tag{23}$$

where $\cos^2\theta = (d_a/R)^2$. Next, by representing Förster radius as the product of distance-dependent and distance-independent terms $R_o = [\kappa^2(R)]^{1/6} \cdot R_o^r$, one obtains

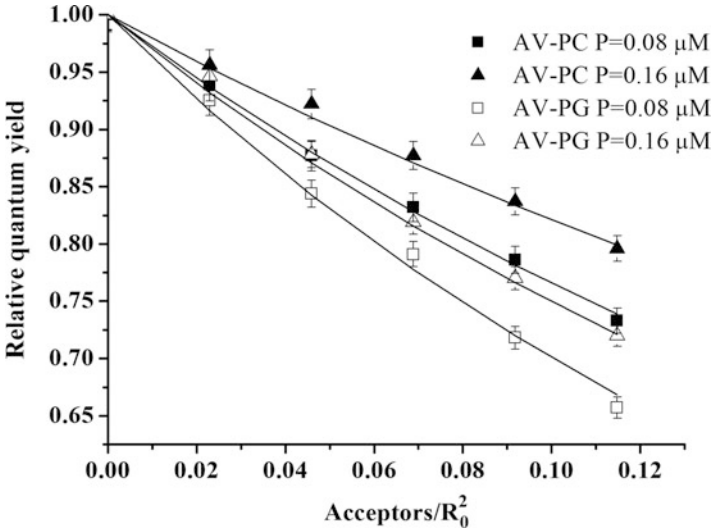

Fig. 4 Förster energy transfer profiles for lysozyme Trp-AV donor-acceptor pair in PC/PG liposomes (40 mol% PG). Lipid concentration was 5 μM

$$S(t) = \int_{d_a}^{\infty} \left[1 - \exp\left(-\lambda\kappa^2(R)\left(\frac{R_o^r}{R}\right)^6\right)\right] 2\pi R dR \tag{24}$$

$$R_o^r = 979\left(n_r^{-4} Q_D J\right)^{1/6}, \quad J = \frac{\int_0^{\infty} F_D(\lambda)\varepsilon_A(\lambda)\lambda^4 d\lambda}{\int_0^{\infty} F_D(\lambda) d\lambda} \tag{25}$$

This formalism was employed to describe FRET between tryptophan residues of lysozyme as donors and anthrylvinyl-labeled phosphatidylcholine (AV-PC) or phosphatidylglycerol (AV-PG) as acceptors in lipid vesicles composed of phosphatidylcholine and varying proportions of phosphatidylglycerol (10, 20, or 40 mol%) [44]. The efficiency of energy transfer was calculated from the sensitized emission of the acceptor by measuring tryptophan fluorescence in the absence and presence of donors. Shown in Fig. 4 are typical dependencies of energy transfer efficiency on the acceptor concentration. AV fluorophore is distributed between the outer and inner membrane leaflets, residing at the level of terminal methyl groups, thus forming two acceptor planes, separated by a certain distance d_t. Taking into account distance dependence of the orientation factor, energy transfer to the outer and inner acceptor planes can be described by the following equations:

$$S_1(\lambda) = \int_{|d_c - 0.5d_t|}^{\infty} \left[1 - \exp\left(-\lambda\kappa_1^2(R)\left(\frac{R_o^r}{R}\right)^6\right)\right] 2\pi R dR \tag{26}$$

$$S_2(\lambda) = \int_{d_c + 0.5d_t}^{\infty} \left[1 - \exp\left(-\lambda\kappa_2^2(R)\left(\frac{R_o^r}{R}\right)^6\right)\right] 2\pi R dR \tag{27}$$

$$\kappa_{1,2}^2(R) = \left\langle d_D^x \right\rangle \left\langle d_A^x \right\rangle \left(3\left(\frac{d_c \mp 0.5d_t}{R}\right)^2 - 1\right) + \frac{1 - \left\langle d_D^x \right\rangle}{3} + \frac{1 - \left\langle d_A^x \right\rangle}{3} + \left(\frac{d_c \mp 0.5d_t}{R}\right)^2 \left(\left\langle d_D^x \right\rangle - 2\left\langle d_D^x \right\rangle \left\langle d_A^x \right\rangle + \left\langle d_A^x \right\rangle\right) \tag{28}$$

$$E = 1 - \int_0^{\infty} \exp(-\lambda) \exp\left[-C_a^s(S_1(\lambda) + S_2(\lambda))\right] d\lambda \tag{29}$$

The relationships 26–29 are valid when the donor and acceptor transition moments are distributed about the axes $\boldsymbol{D_x}$ and $\boldsymbol{A_x}$ parallel to the bilayer normal $\boldsymbol{N}$. If this is not the case, additional depolarization factors accounting for the deviations of $\boldsymbol{D_x}$ and $\boldsymbol{A_x}$ from $\boldsymbol{N}$ should be introduced: $d_{D,A}^a = \frac{3}{2}\cos^2\alpha_{D,A} - \frac{1}{2}$, where $\alpha_{D,A}$ are the angles made by $\boldsymbol{D_x}$ and $\boldsymbol{A_x}$ with $\boldsymbol{N}$. By applying the Soleillet's theorem stating the multiplicativity of depolarization factors, Eq. 28 may be rewritten in a more general form

$$\kappa_{1,2}^2(R) = d_D d_A \left(3\left(\frac{d_c \mp 0.5d_t}{R}\right)^2 - 1\right) + \frac{1 - d_D}{3} + \frac{1 - d_A}{3} + \left(\frac{d_c \mp 0.5d_t}{R}\right)^2 (d_D - 2d_D d_A + d_A) \tag{30}$$

where $d_{D,A} = \left\langle d_{D,A}^x \right\rangle d_{D,A}^a$. Allowing for the size of AV fluorophore (ca. 0.7 × 0.3 nm) and high mobility of the terminal groups of hydrocarbon chains, d_t value was slightly varied in the range from 0.3 to 0.7 nm, while parameter d_c, characterizing the distance between the donor plane and membrane center, was optimized in the data-fitting procedure. The axial depolarization factors were calculated using the results of steady-state fluorescence anisotropy measurements. The recovered values of the donor separation from bilayer center are consistent with the location of lysozyme Trp residues in the interfacial bilayer region. Our data agree with the viewpoint that helix-loop-helix domain (87–114 residues) located at the upper lip of the active site cleft accounts for lysozyme insertion into lipid bilayer. The nonpolar portion of this domain (residues 87–95) penetrating into hydrophobic bilayer region

serves as a membrane anchor, while terminal basic residues form electrostatic contacts with anionic phospholipid headgroups. This mode of membrane binding of lysozyme causes Trp62 and Trp108 to be accommodated at the interface.

This example demonstrates that for donors and acceptors residing at different depths within the membrane, orientation factor can be incorporated as a distance-dependent parameter at the integration over R step in the theoretical calculation of FRET efficiency. Knowing the steady-state and fundamental anisotropies of donor and acceptor, allows to raise the accuracy of FRET-based estimates of the transverse location of membrane-associated proteins.

6 FRET in Characterization of Protein-Lipid Binding

A specific feature of energy transfer in membranes is the dependence of FRET efficiency on acceptor surface concentration (Eq. 17). This makes FRET technique suitable for determination of not only structural parameter (position relative to lipid-water interface) but also the binding parameters (association constant and the number of lipids per bound protein) [47–49]. In the case when acceptor is intrinsic or extrinsic protein chromophore, for example, tryptophan residue or heme group, and protein is distributed between aqueous and lipid phases, the amount of membrane-bound acceptor (B_a) can be related to the total acceptor concentration (A), using the appropriate binding model. In terms of conventional Langmuir model, this relationship is given by

$$K_a = \frac{B_a}{(A - B_a)(L_a/n - B_a)},$$
$$B_a = \frac{1}{2}\left[A + \frac{L_a}{n} + \frac{1}{K_a} - \sqrt{\left(A + \frac{L_a}{n} + \frac{1}{K_a}\right)^2 - 4\frac{AL_a}{n}}\right] \tag{31}$$

where K_a is the equilibrium association constant and n is the binding stoichiometry.

By combining the FRET and binding models, one obtains the relative quantum yield as a function of five variables $Q_r = f(A, L_a, K_a, n, d_c)$. Of these, total acceptor concentration, A, and amount of accessible lipid L_a(usually taken as a half of total lipid concentration for large unilamellar vesicles and nonpermeating acceptor) are independent parameters that can be varied in the experiment, while K_a, n, and d_c are unknown parameters which can be derived from least-squares fitting of the experimental data. However, unambiguous evaluation of the structural and binding characteristics is complicated by a strong cross-correlation between optimizing parameters, which makes it impossible to judge whether the changes in donor quantum yield result from the variation of the acceptor transverse location or from alterations in the extent of its association with the membrane. To overcome this problem, we have tried to ascertain what format of FRET measurements

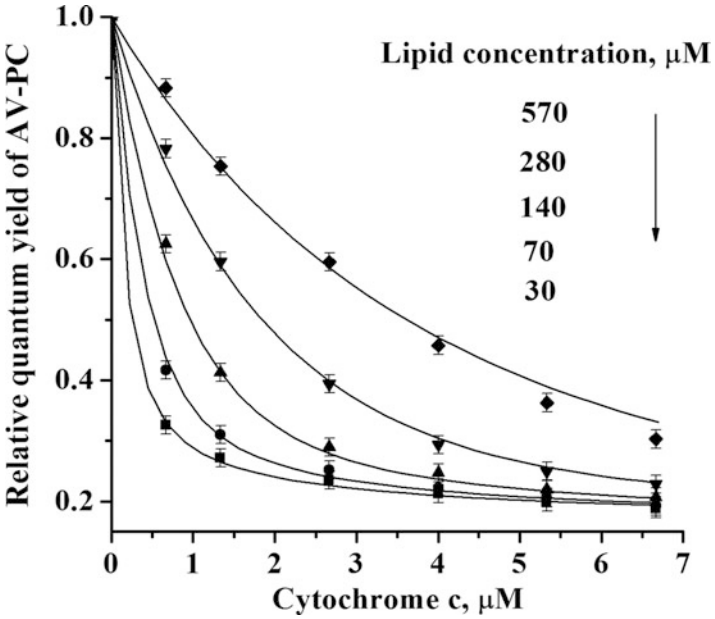

Fig. 5 Förster energy transfer profiles for cytochrome *c* heme-AV donor-acceptor pair in PC/CL liposomes (10 mol% CL)

permits unequivocal resolution of the structural and binding parameters [50]. Using computer simulations relative quantum yield of a donor was calculated in terms of the above analytical model for various combinations of acceptor (A) and lipid concentrations (L) with preset values of optimizing parameters K_a, n, and d_c. Gaussian noise was added to the calculated data to mimic the experimental errors. Three characteristic FRET datasets were analyzed: (1) univariate data (1D data) obtained at a fixed lipid concentration by varying total acceptor concentration only, (2) two-dimensional data array (2D data) obtained by varying both lipid and total acceptor concentrations for the case of saturable binding, and (3) 2D data for the case of unsaturable binding. To assess how the quality and uniqueness of the least-squares fitting depend on the format of FRET data, we analyzed the projections of the corresponding error surfaces (χ^2 statistic for a given dataset) with respect to a specific parameter. Simulation results clearly indicated that only analysis of two-dimensional data arrays with saturable binding allows the model parameters to be recovered with high accuracy and statistical significance.

The proposed global analysis approach has been employed to analyze FRET between anthrylvinyl-labeled phosphatidylcholine (AV-PC) as an energy donor and heme group of cytochrome *c* as an acceptor [50]. AV-PC was incorporated into lipid vesicles composed of phosphatidylcholine and 10 mol% of cardiolipin (CL). AV fluorophore is localized in a lipid bilayer close to the terminal methyl groups, preferentially orienting parallel to the lipid acyl chains. Shown in Fig. 5 is relative

quantum yield of AV-PC as a function of the total cytochrome *c* concentration, recorded at five different lipid concentrations. As the lipid concentration increases, acceptor molecules tend to distribute over a greater bilayer area resulting in the decrease of acceptor surface concentration and lowered energy transfer. It is this peculiarity of energy transfer dependence on total acceptor and lipid concentrations that makes it possible to resolve structural and binding parameters by the least-squares fitting of the expanded data array. Solid lines in Fig. 5 represent best fit of the FRET data by the global analysis procedure yielding the following estimates of the fitting parameters: $d_c = 3.6 \pm 0.2$, nm; $K_a = 3.6 \pm 1.1$, μM^{-1}; and $n = 27 \pm 2$. Thus, in the case where energy transfer occurs from donors localized in the membrane at a known depth to acceptors distributed between aqueous and lipid phases, analysis of two-dimensional data arrays can provide unambiguous information on both binding parameters and transverse membrane location of protein fluorophore.

The above example reflects only one of the possibilities offered by FRET technique in elucidating the quantitative and qualitative aspects of protein-lipid binding. Most of these aspects are highlighted in the brilliant recent works from Loura and Prieto group [51–54]. The authors discuss how FRET may help in establishing protein preference to a certain type of lipids and make a critical comparison of the existing theoretical approaches to quantification of protein-lipid selectivity.

7 Protein Aggregation in a Membrane Environment Detected by FRET

FRET has been conventionally used in membrane studies for monitoring the changes in protein aggregation state [55–58]. The enhancement of energy transfer between protein derivatives fluorescently labeled with donor and acceptor is regarded as a qualitative proof of protein self-association. Further quantitative analysis can, in principle, yield the estimates of aggregate size using appropriate data treatment formalism. To perform such kind of analysis most correctly, it is important to differentiate FRET between donors and acceptors confined to protein aggregates from energy transfer involving nonaggregated species [54]. The contribution of this interfering FRET can be neglected only in the case of very low concentration of the tagged protein. Furthermore, fluorescent labeling can modify self-associating propensity of polypeptide chain [59]. Along with the complexity of aggregation process per se, these factors may limit the amount of reliable quantitative information on oligomeric structure. A versatility of the problems addressed by FRET in the field of protein aggregation is illustrated by a number of works reviewed, particularly, in [3]. To exemplify, in the pioneering work of Vanderkooi et al., Ca^{2+} ATPase of sarcoplasmic reticulum was covalently labeled with *N*-iodoacetyl-*N*′-(5-sulfo-naphthyl)ethylenediamine (IAEDANS) as a donor and

iodoacetamidofluorescein (IAF) as an acceptor [60]. While analyzing the results of FRET measurements in reconstituted vesicles, the authors reasonably considered two possibilities: (1) energy transfer occurring when the donor- and acceptor-tagged molecules collide or come within the Förster distance due to Brownian motion and (2) energy transfer in ATPase oligomers in which the donor and acceptor come into close proximity. The observations that FRET was not altered with increasing lipid-to-protein molar ratio but was abolished by the addition of unlabeled protein have been regarded as the arguments in favor of ATPase self-association. By measuring energy transfer between Trp and its nonfluorescent 2-hydroxy-5-nitrobenzylbromide (HNB) derivative, John and Jahnig obtained evidence for melittin aggregation in dimyristoylphosphatidylcholine (DMPC) bilayer [61]. Investigation of FRET between fluorescent tags 2,6-dansyl chloride and dabsyl chloride led Adair and Engelman to conclusion that peptide mimicking transmembrane region of glycophorin A forms helical dimers in DMPC model membranes [62]. Using the formalism of site-directed cross-linking approach to the determination of oligomeric structure [63] and assuming equal energy transfer to all subunits in oligomer, the authors proposed the method allowing to distinguish dimers from higher oligomers. The linear dependence of FRET efficiency on acceptor mole fraction was shown to be a characteristic sign of dimer formation. Further steps to solving this problem have been made by Li et al. [64]. A simulation-based approach was developed to resolve the number of subunits in oligomer, the distance between labeled sites on different subunits, and the fraction of monomers. This approach was used to characterize the oligomeric structure of phospholamban (PLB) in dioleoylphosphatidylcholine (DOPC) bilayer.

Sparr et al. employed FRET technique to ascertain how lipid bilayer thickness affects the aggregation propensity of a series of Trp-flanked peptides specifically tagged with pyrene [65]. Analysis of energy transfer from Trp to pyrene indicated that hydrophobic mismatch promotes helix-helix association. Using fluorescent labels 5-((2-aminoethyl)amino) naphthalene-1-sulfonic acid (EDANS) as a donor and fluorescein isothiocyanate (FITC) as an acceptor, Fernandes et al. obtained the arguments in favor of membrane-mediated dimerization of N-terminal amphipathic α-helix peptide (H0-NBAR) of the BAR (Bin, amphiphysin, Rvs) domain. It was demonstrated that simultaneous fitting of two datasets corresponding to different lipid/protein ratios permits quantification of the FRET contributions from aggregated and nonaggregated peptide [66]. FRET measurements performed by Fung and coworkers with Cy3-Cy5 donor-acceptor pair offered insights into the mechanisms of membrane-mediated oligomerization of β_2-adrenoceptor [67]. Tetrameric species of this protein were hypothesized to dominate in the lipid bilayer from DOPC and cholesterol hemisuccinate.

One of the main tendencies in the past decade is the increasing use of FRET in monitoring the process of protein aggregation in vivo. For instance, Rajan et al. found evidence for high specificity of protein-protein interactions in living cell [68]. For this purpose, aggregation-prone proteins were biosynthetically tagged with

mutant forms of green fluorescent protein (GFP), cyan (CFP), and yellow fluorescent proteins (YFP), with spectral overlap suitable for FRET. Similar donor-acceptor pair was employed by Mihai et al. who investigated oligomerization of discoidin domain receptor on the cell surface [69] and Woehler et al. who analyzed the oligomeric state of the 5-HT1A receptor within living cells [70]. Liu and coauthors recruited GFP as a donor and red fluorescence protein (RFP) as an acceptor in confocal FRET microscopy study of T5P gC-crystallin aggregation in cell cytoplasm [71].

Remarkably, combined use of different FRET formats allows determining the structure of complex protein-lipid aggregates, as was demonstrated in recent studies of Coutinho et al. [72, 73]. By measuring energy transfer in two types of donor-acceptor pairs, involving BODIPY-labeled lipid or Alexa-488-labeled protein as donors and rhodamine-labeled lipids as acceptors, the authors succeeded in structural characterization of supramolecular aggregates formed by lysozyme and negatively charged membranes. The recovered pinched multilamellar motif was hypothesized to govern the structure of amyloid-like fibrils found in protein-lipid systems.

8 Protein-Induced Lipid Demixing Monitored by FRET

Another essential aspect in which FRET technique may prove useful concerns membrane heterogeneity, viz., lipid lateral redistribution in response to protein binding followed by domain formation [74, 75]. Two underlying processes are considered: (1) local lipid demixing implicating molecular-scale deviation from the average lipid composition within and around the protein-membrane interaction zone and (2) the formation of macroscopic protein-lipid domains enriched in specific lipid [76, 77]. The characteristic distance scale of energy transfer makes this technique particularly sensitive to nanometer-size domains. Pros and cons of different approaches to FRET analysis of lateral membrane domains are given in exhaustive recent reviews [15, 78]. Therefore, here, we restrict ourselves to simplest illustrations of how steady-state FRET can be used to detect domain formation in the model protein-lipid systems.

We employed FRET to define demixing-favoring conditions and the extent of lipid redistribution produced by the basic proteins lysozyme and cytochrome *c* in the binary negatively charged model membranes composed of PC and PG [44, 79]. To answer the question of whether these proteins are capable of inducing the formation of lateral domains enriched in anionic lipids, we compared energy transfer efficiencies in the systems containing either AV-PC or AV-PG as energy acceptors for lysozyme tryptophans or energy donors for heme group of cytochrome *c*. As shown in Fig. 4, the use of AV-PG instead of AV-PC as energy acceptor for tryptophan residues of lysozyme resulted in higher efficiencies of energy transfer. This finding can be interpreted in terms of lysozyme ability to promote lipid lateral redistribution followed by the accumulation of anionic lipid in

the vicinity of bound protein. As positively charged lysozyme approaches the membrane surface, PG molecules migrate toward interaction zone, thereby replacing PC molecules. To describe this process, the FRET model considered above was complemented by two additional parameters, characterizing the radius of lateral domains (r_{dm}) and the ratio of PG concentrations in the interaction zone at nonrandom and random acceptor distribution (k). Thus, the expressions for FRET efficiency take the following form:

$$E = 1 - \int_0^{\infty} \exp(-\lambda) \exp\left[-C_a^s \left(\left[\frac{L_{out}S_L - Pf_b\pi r_{dm}^2 k}{L_{out}S_L - Pf_b\pi r_{dm}^2}\right] S_{11}(\lambda) + kS_{12}(\lambda) + S_2(\lambda)\right)\right] d\lambda \tag{32}$$

$$S_{11}(\lambda) = \int_{\left[r_{dm}^2 + (d_c - 0.5d_t)^2\right]^{0.5}}^{\infty} \left[1 - \exp\left(-\lambda\kappa_1^2(R)\left(\frac{R_o^r}{R}\right)^6\right)\right] 2\pi R dR \tag{33}$$

$$S_{12}(\lambda) = \int_{|d_c - 0.5d_t|}^{\left[r_{dm}^2 + (d_c - 0.5d_t)^2\right]^{0.5}} \left[1 - \exp\left(-\lambda\kappa_1^2(R)\left(\frac{R_o^r}{R}\right)^6\right)\right] 2\pi R dR \tag{34}$$

Here L_{out} is the lipid concentration in the outer monolayer, $f_b = B/P$ is the fraction of bound protein, B is the molar concentration of bound protein, and P is the total protein concentration. The FRET profiles obtained with AV-PG as energy acceptor were approximated by Eqs. 32–34, using the following data treatment strategy: (1) parameter k was allowed to vary from 1 to its maximum value (2.5) possible for the model membranes under study, in which PG proportion was 40 mol%; (2) parameter r_{dm} was taken from the limits dictated by the requirement that the area occupied by protein-induced lateral domains must be less than the total membrane area $Pf_b\pi r_{dm}^2 k \le L_{out}S_L$; and (3) parameter d_c, denoting the distance between the plane of donors, that is, lysozyme tryptophan residues, and membrane midplane, was optimized for every pair of r_{dm} and k. In this way, we recovered the sets $\{r_{dm},\ k,\ d_c\}$ providing the best fit of the experimental data. Good agreement between theory and experiment was found for conditions where size of the region with increased PG concentration (r_{dm}) was less than 3.4 nm. The fact that this estimate is comparable with lysozyme radius (ca. 3 nm) is indicative of a local deviation from the average lipid composition.

Analogous conclusion was reached for another basic protein – cytochrome c using simulation-based data analysis methodology. We examined FRET between AV-PC or AV-PG as donors and the heme group of cytochrome c as an acceptor in PC/PG model membranes containing 10-, 20-, or 40-mol% PG [79]. The differences between AV-PC and AV-PG FRET profiles were observed only at PG content 10 mol%, suggesting a segregation of anionic lipids into lateral domains.

To interpret this effect quantitatively, the Monte-Carlo simulation was designed, in which AV-PG donors were considered as being randomly distributed within disk-shaped domains centered at each acceptor location. Our main goal was to determine characteristic domain size, that is, dimension of the protein-affected region where PG concentration is k times higher than that for a random lipid distribution. Positions of donors and acceptors were generated randomly in a square cell with the side length taken as $10R_o$, assuming periodic boundary conditions to avoid edge effects. The relative quantum yield averaged over all donors was calculated from the fluorophore coordinates using the following equation:

$$Q_r = \frac{1}{N_D}\sum_{j=1}^{N_D}\left[1+\sum_{i=1}^{N_{AC}}\left(\frac{R_o^r\kappa^2(r_{ij})}{r_{ij}}\right)^6\right]^{-1} \tag{35}$$

where N_D, N_{AC} stand for the number of donors and acceptors in a square cell. The number of acceptors was determined by multiplying protein surface density by the cell square. By operating with the quantities, such as domain radius, the ratio of PG concentrations in the domain region at nonrandom and random distribution of charged lipids and total number of disk-shaped domains, which was taken equal to the number of membrane-bound protein molecules, we calculated the number of donors (i.e., AV-PG or AV-PC) in domain and nondomain regions of a cell. The simulation procedure was repeated for multiple fluorophore configurations until the standard deviation in relative quantum yield was less than 2 %. Simulation-based fitting of the FRET data with k being varied from 1 to 10 (the value corresponding to complete replacement of PC with PG) revealed domain radius not to exceed 4 nm, implying that cytochrome-induced lipid demixing takes place locally, in the immediate vicinity of the adsorbed protein.

9 Concluding Remarks

The past few decades have seen tremendous upsurge in the use of FRET technique in biomedical studies, especially in structural characterization of membrane systems. This chapter illuminates only a minor fraction of FRET applications in this research area. Our goal was to illustrate that even the simplest steady-state formats of FRET measurements feasible for most laboratories can provide valuable information about the structure of protein-lipid assemblies. FRET between multiple donors and acceptors distributed in lipid phase or confined to membrane-associated protein molecules can be described analytically only for the case of random fluorophore distribution. Therefore, the accent is now shifting toward the development of simulation-based data analysis approaches, particularly, Monte-Carlo simulations, which offer much more versatility and can be applied for any complex geometric conditions [80, 81]. Another recent trend is the extension of time-resolved FRET measurements having serious advantages in determining the size

of lateral membrane domains [15]. Nevertheless, potential of steady-state FRET is far from being fully exhausted. The above examples demonstrate that this kind of FRET may prove useful in answering the questions of (1) whether there exists certain specific orientation of the protein molecule relative to lipid-water interface; (2) what is the transverse membrane location of protein fluorophores; (3) what are the protein-membrane binding characteristics; (4) how membrane environment affects protein aggregation state; and (5) whether lipid molecules undergo lateral redistribution in response to protein adsorption.

In general, the most sensible experimental strategies for FRET-based analysis of protein-lipid interactions seem to lie in correlating the data from a multitude of donor-acceptor pairs (involving both intrinsic and extrinsic protein fluorophores and lipid tags with defined bilayer location) and different formats of FRET measurements. The perspectives of FRET are associated with synergistic progress in the development of novel (1) instrumentation and more sophisticated data treatment methods, (2) genetically encoded fluorescent proteins and site-specific fluorescent labels, and (3) fluorophores with improved characteristics (higher signal/background noise ratio and photostability, smaller size, wider range of excited state lifetimes). There is no doubt that continuous refinement of FRET technique will substantially expand the area of its application in membrane studies.

Acknowledgments GG gratefully acknowledges a visiting scientist award by the Sigrid Juselius Foundation. This work was supported by the grants from European Social Fund (project number 2009/0205/1DP/1.1.1.2.0/09/APIA/VIAA/152) and Fundamental Research State Fund of Ukraine (project number F.41.4/014).

References

1. Selvin PR (2000) The renaissance of fluorescence resonance energy transfer. Nat Struct Biol 7:730–734
2. Giepmans BNG, Adams SR, Ellisman MH, Tsien RY (2006) The fluorescent toolbox for assessing protein location and function. Science 312:217–224
3. Loura LMS, Prieto M (2011) FRET in membrane biophysics: an overview. Front Physiol. doi:10.3389/fphys.2011.00082
4. Wu P, Brand L (1994) Resonance energy transfer: methods and applications. Anal Biochem 218:1–13
5. Selvin PR (1995) Fluorescence resonance energy transfer. Method Enzymol 246:300–334
6. Matko J, Edidin M (1997) Energy transfer methods in detecting molecular clusters on cell surfaces. Method Enzymol 278:444–462
7. Wong AP, Groves JT (2002) Molecular topography imaging by intermembrane fluorescence resonance energy transfer. Proc Natl Acad Sci U S A 99:14147–14152
8. Hoppe A, Christensen K, Swanson JA (2002) Fluorescence resonance energy transfer-based stoichiometry in living cells. Biophys J 83:3652–3664
9. Subramanian M, Jutila A, Kinnunen PKJ (1998) Binding and dissociation of cytochrome c to and from membranes containing acidic phospholipids. Biochemistry 37:1394–1402

10. Corbalan-Garcia S, Sanchez-Carrillo S, Garcia-Garcia J, Gomez-Fernandez JC (2003) Characterization of the membrane binding mode of the C2 domain of PKCε. Biochemistry 42:11661–11668
11. Calleja V, Ameer-Beg SM, Vojnovic B, Woscholski R, Downward J, Larijani B (2003) Monitoring conformational changes of proteins in cells by fluorescence lifetime imaging microscopy. Biochem J 372:33–40
12. Chigaev A, Buranda T, Dwyer DC, Prossnitz ER, Sklar LA (2003) FRET detection of cellular α_4-integrin conformational activation. Biophys J 85:3951–3962
13. Yano Y, Takemoto T, Kobayashi S, Yasui H, Sakurai H, Ohashi W, Niwa M, Futaki S, Sugiura Y, Matsuzaki K (2002) Topological stability and self-association of a completely hydrophobic model transmembrane helix in lipid bilayers. Biochemistry 41:3073–3080
14. You M, Li E, Wimley WC, Hristova K (2005) Förster resonance energy transfer in liposomes: measurements of transmembrane helix dimerization in the native bilayer environment. Anal Biochem 340:154–164
15. Loura LMS, Fernandes F, Prieto M (2010) Membrane microheterogeneity: Förster resonance energy transfer characterization of lateral membrane domains. Eur Biophys J 39:589–607
16. Brown AC, Towles KB, Wrenn SP (2007) Measuring raft size as a function of membrane composition in PC-based systems: part I- binary systems. Langmuir 23:11180–11187
17. Scholes GD (2003) Long-range resonance energy transfer in molecular systems. Annu Rev Phys Chem 54:57–87
18. Förster T (1948) Intermolecular energy migration and fluorescence. Ann Phys 2:55–75
19. Lakowicz JR (1999) Principles of fluorescence spectroscopy. Kluwer/Plenum, New York
20. Valeur B (2001) Molecular fluorescence: principles and applications. Wiley-VCH Verlag GmbH, Weinheim
21. Fung B, Stryer L (1978) Surface density determination in membranes by fluorescence energy transfer. Biochemistry 17:5241–5248
22. Estep T, Thompson T (1979) Energy transfer in lipid bilayers. Biophys J 26:195–208
23. Wolber P, Hudson B (1979) An analytic solution to the Förster energy transfer problem in two dimensions. Biophys J 28:197–210
24. Dewey T, Hammes G (1980) Calculation of fluorescence resonance energy transfer on surfaces. Biophys J 32:1023–1036
25. Snyder B, Freire E (1982) Fluorescence energy transfer in two dimensions. A numeric solution for random and nonrandom distributions. Biophys J 40:137–148
26. Doody M, Sklar L, Pownall H, Sparrow J, Gotto A, Smith L (1983) A simplified approach to resonance energy transfer in membranes, lipoproteins and spatially restricted systems. Biophys Chem 17:139–152
27. Gutierrez-Merino G, Munkonge F, Mata A, East J, Levinson B, Napier R, Lee A (1987) The position of ATP binding site on the (Ca^{2+} + Mg^{2+})-ATPase. Biochim Biophys Acta 897:207–216
28. Dale R, Eisinger J, Blumberg W (1979) The orientational freedom of molecular probes. The orientation factor in intramolecular energy transfer. Biophys J 26:161–194
29. Gorbenko GP (1999) Structure of cytochrome c complexes with phospholipids as revealed by resonance energy transfer. Biochim Biophys Acta 1420:1–13
30. Dickerson RE, Takano T, Eisenberg D, Kallai OB, Samson L, Cooper A, Margoliash E (1971) Ferricytochrome c. General features of the horse and bonito proteins at 2.8 Å resolution. J Biol Chem 246:1511–1535
31. Nazarov PV, Koehorst RB, Vos WL, Apanasovich VV, Hemminga MA (2006) FRET study of membrane proteins: simulation-based fitting for analysis of membrane protein embedment and association. Biophys J 91:454–466
32. Lehto MT, Sharom FJ (2002) Proximity of the protein moiety of a GPI-anchored protein to the membrane surface: a FRET study. Biochemistry 41:8368–8376
33. Antollini SS, Soto MA, de Romanelli IB, Gutierrez-Merino C, Sotomayor P (1996) Physical state of bulk and protein-associated lipid in nicotinic acetylcholine receptor-rich membrane

studied by laurdan generalized polarization and fluorescence energy transfer. Biophys J 70:1275–1284
34. Barrera FN, Poveda JA, Gonzalez-Ros JM, Neira JL (2003) Binding of the C-terminal sterile α motif (SAM) domain of human p73 to lipid membranes. J Biol Chem 278:46878–46885
35. Ramachandran R, Tweten RK, Johnson AE (2005) The domains of a cholesterol-dependent cytolysin undergo a major FRET-detected rearrangement during pore formation. Proc Natl Acad Sci U S A 102:7139–7144
36. Kleinfeld AM, Lukacovic MF (1985) Energy transfer study of cytochrome b5 using the anthroyloxy fatty acid membrane probes. Biochemistry 24:1883–1890
37. Ward RJ, Palmer M, Leonard K, Bhakdi S (1994) Identification of a putative membrane-inserted segment in the α -toxin of *Staphylococcus aureus*. Biochemistry 33:7411–7484
38. Liu R, Sharom FJ (1998) Proximity of the nucleotide binding domains of the P-glycoprotein multidrug transporter to the membrane surface: a resonance energy transfer study. Biochemistry 37:6503–6512
39. Shaklai N, Yguerabide J, Ranney HM (1977) Interaction of hemoglobin with red blood cell membranes as shown by a fluorescent chromophore. Biochemistry 16:5585–5592
40. Munkonge F, East JM, Lee AG (1989) Positions of the sites labeled by *N*-cyclohexyl-*N*′-(4-dimethylamino-1-naphthyl)carbodiimide on the (Ca^{2+} + Mg^{2+})-ATPase. Biochim Biophys Acta 979:113–120
41. Johnson DA, Nuss JM (1994) The histrionicotoxin-sensitive ethidium binding site is located outside of the transmembrane domain of the nicotinic acetylcholine receptor: a fluorescence study. Biochemistry 33:9070–9077
42. Remmers AE, Neubig RR (1993) Resonance energy transfer between guanine nucleotide binding protein subunits and membrane lipids. Biochemistry 32:2409–2414
43. Carraway KL, Koland JG, Cerione RA (1990) Location of the epidermal growth factor binding site on the EGF receptor. A resonance energy transfer study. Biochemistry 29:8741–8747
44. Gorbenko GP, Ioffe VM, Molotkovsky JG, Kinnunen PKJ (2008) Resonance energy transfer study of lysozyme-lipid interactions. Biochim Biophys Acta 1778:1213–1221
45. Gorbenko GP, Molotkovsky JG, Kinnunen PKJ (2006) Cytochrome c interaction with cardiolipin/phosphatidylcholine model membranes: effect of cardiolipin protonation. Biophys J 90:4093–4103
46. Davenport L, Dale R, Bisby R, Cundall R (1985) Transverse location of the fluorescent probe 1,6-diphenyl-1,3,5-hexatriene in model lipid bilayer membrane systems by resonance excitation energy transfer. Biochemistry 24:4097–4108
47. Dorn IT, Neumaier KR, Tampe R (1998) Molecular recognition of histidine-tagged molecules by metal-chelating lipids monitored by fluorescence energy transfer and correlation spectroscopy. J Am Chem Soc 120:2753–2763
48. Wang T, Pentyala S, Rebecchi MJ, Scarlata S (1999) Differential association of the pleckstrin homology domains of phospholipases C-β_1, C-β_2, and C-δ_1 with lipid bilayers and the βγ subunits of heterotrimeric G proteins. Biochemistry 38:1517–1524
49. Komander D, Fairservice A, Deak M, Kular GS, Prescott AR, Downes CP, Safrany ST, Alessi DR, van Aalten DMF (2004) Structural insights into the regulation of PDK1 by phosphoinositides and inositol phosphates. EMBO J 23:3918–3928
50. Domanov YA, Gorbenko GP, Molotkovsky JG (2004) Global analysis of steady-state energy transfer measurements in membranes: resolution of structural and binding parameters. J Fluoresc 14:49–55
51. Fernandes F, Loura LMS, Koehorst R, Spruijt RB, Hemminga M, Fedorov A, Prieto M (2004) Quantification of protein-lipid selectivity using FRET: application to the M13 major coat protein. Biophys J 87:344–352
52. Capeta RC, Poveda JA, Loura LMS (2006) Non-uniform membrane probe distribution in resonance energy transfer: application to protein-lipid selectivity. J Fluoresc 16:161–172

53. Picas L, Suarez-Germa C, Montero MT, Vazquez-Ibar JL, Hernandez-Borrell JH, Prieto M, Loura LMS (2010) Lactose permease lipid selectivity using Förster resonance energy transfer. Biochim Biophys Acta 1798:1707–1713
54. Loura LMS, Prieto M, Fernandes F (2010) Quantification of protein-lipid selectivity using FRET. Eur Biophys J 39:565–578
55. Hillger F, Nettels D, Dorsch S, Schuler B (2007) Detection and analysis of protein aggregation with confocal single molecule fluorescence spectroscopy. J Fluoresc 17:759–765
56. Li E, You M, Hristova K (2005) Sodium dodecyl sulfate – polyacrylamide gel electrophoresis and Förster resonance energy transfer suggest weak interactions between fibroblast growth factor receptor 3 (FGFR3) transmembrane domains in the absence of extracellular domains and ligands. Biochemistry 44:352–360
57. Floyd DH, Geva A, Bruinsma SP, Overton MC, Blumer KJ, Baranski TJ (2003) C5a receptor oligomerization. II. Fluorescence resonance energy studies of a human G protein-coupled receptor expressed in yeast. J Biol Chem 278:35354–35361
58. Agirre A, Barco A, Carrasco L, Nieva JL (2002) Viroporin-mediated membrane permeabilization: pore formation by nonstructural poliovirus 2B protein. J Biol Chem 277:40434–40441
59. Moens PDJ, Yee DJ, Remedios CG (1994) Determination of the radial coordinate of Cys-374 in F-actin using fluorescence resonance energy transfer spectroscopy: effect of phalloidin on polymer assembly. Biochemistry 33:13102–13108
60. Vanderkooi JM, Ierokomas A, Nakamura H, Martonosi A (1977) Fluorescence energy transfer between Ca^{2+} transport ATPase molecules in artificial membranes. Biochemistry 16:1262–1267
61. John E, Jahnig F (1991) Aggregation state of melittin in lipid vesicle membranes. Biophys J 60:319–328
62. Adair BD, Engelman DM (1994) Glycophorin A helical transmembrane domains dimerize in phospholipid bilayers: a resonance energy transfer study. Biochemistry 33:5539–5544
63. Milligan DL, Koshland DE (1988) Site-directed cross-linking: establishing the dimeric structure of the aspartate receptor of bacterial chemotaxis. J Biol Chem 263:6268–6275
64. Li M, Reddy LG, Bennett R, Silva ND, Jones LR, Thomas DD (1999) A fluorescence energy transfer method for analyzing protein oligomeric structure: application to phospholamban. Biophys J 76:2587–2599
65. Sparr E, Ash WL, Nazarov PV, Rijkers DT, Hemminga MA, Tieleman DP, Killian JA (2005) Self-association of transmembrane-helices in model membranes: importance of helix orientation and role of hydrophobic mismatch. J Biol Chem 280:39324–39331
66. Fernandes F, Loura LMS, Chichon FJ, Carrascosa JL, Fedorov A, Prieto M (2008) Role of helix 0 of the N-BAR domain in membrane curvature generation. Biophys J 94:3065–3073
67. Fung JJ, Deup X, Pardo L, Yao XJ, Velez-Ruiz GL, DeVree BT, Sunahara RK, Kobilka BK (2009) Ligand-regulated oligomerization of β2-adrenoceptors in a model lipid bilayer. EMBO J 28:3315–3328
68. Rajan SR, Illing ME, Bence NF, Kopito RR (2001) Specificity in intracellular protein aggregation and inclusion body formation. Proc Natl Acad Sci U S A 98:13060–13065
69. Mihai C, Chotani M, Elton TS, Agarwal G (2009) Mapping of DDR1 distribution and oligomerization on the cell surface by FRET microscopy. J Mol Biol 385:432–445
70. Woehler A, Wlodarczyk J, Ponimaskin EG (2009) Specific oligomerization of the 5-HT1A receptor in the plasma membrane. Glycoconj J 26:749–756
71. Liu BF, Song S, Hanson M, Liang JJN (2008) Protein-protein interactions involving congenital cataract T5P gC-crystallin mutant: a confocal fluorescence microscopy study. Exp Eye Res 87:515–520
72. Coutinho A, Loura LMS, Fedorov A, Prieto M (2008) Pinched multilamellar structure of aggregates of lysozyme and phosphatidylserine-containing membranes revealed by FRET. Biophys J 95:4726–4736

73. Coutinho A, Loura LMS, Prieto M (2011) FRET studies of lipid-protein aggregates related to amyloid-like fibers. J Neurochem 116:696–701
74. Kenworthy AK, Petranova N, Edidin M (2000) High-resolution FRET microscopy of cholera toxin B-subunit and GPI-anchored proteins in cell plasma membranes. Mol Biol Cell 11:1645–1655
75. Loura LMS, de Almeida RFM, Prieto M (2001) Detection and characterization of membrane microheterogeneity by resonance energy transfer. J Fluoresc 11:197–209
76. Sperotto MM, Mouritsen OG (1993) Lipid enrichment and selectivity of integral membrane proteins in two-component lipid bilayers. Eur Biophys J 22:323–328
77. Mbamala EC, Ben-Shaul A, May S (2005) Domain formation induced by the adsorption of charged proteins on mixed lipid membranes. Biophys J 88:1702–1714
78. Loura LMS, de Almeida RFM, Silva LC, Prieto M (2009) FRET analysis of domain formation and properties in complex membrane systems. Biochim Biophys Acta 1788:209–224
79. Gorbenko GP, Trusova VM, Molotkovsky JG, Kinnunen PKJ (2009) Cytochrome c induces lipid demixing in weakly charged phosphatidylcholine/phosphatidyl-glycerol model membranes as evidenced by resonance energy transfer. Biochim Biophys Acta 1788: 1358–1365
80. Berney C, Danuser G (2003) FRET or no FRET: a quantitative comparison. Biophys J 84:3992–4010
81. Corry B, Jayatilaka D, Rigby P (2005) A flexible approach to the calculation of resonance energy transfer efficiency between multiple donors and acceptors in complex geometries. Biophys J 89:3822–3836